Many-body perturbation-theory calculations of energy levels along the lithium isoelectronic sequence

W. R. Johnson, S. A. Blundell, and J. Sapirstein
Department of Physics, University of Notre Dame, Notre Dame, Indiana 46556
(Received 6 August 1987)

Energies of $n=2$ states for ions of the lithium isoelectronic sequence are calculated from $Z=3-92$, starting from a Hartree-Fock potential and including second- and third-order correlation corrections, the lowest-order Breit interaction with retardation treated exactly, the second-order correlation corrections to the Breit interaction, and corrections for reduced mass and mass polarization. The resulting differences between theory and experiment for the $2p$ fine structure and the $2s$-$2p$ splittings are found to be in rough agreement with the one-electron Lamb shift, but clear deviations can be seen. A discussion is given of the calculations required to evaluate these deviations within the framework of quantum electrodynamics.

I. INTRODUCTION

The lack of highly accurate calculations of properties of many-electron atoms limits the interpretation in terms of fundamental physics of the increasingly accurate experimental studies of these systems. A notable example is the uncertainty in the atomic calculations of parity nonconservation in heavy atoms,[1] where the accuracy of information about the weak interactions that can be extracted from the most accurate measurement is limited by the uncertainty in the atomic calculations. Another example, which forms the subject matter of this paper, is testing the underlying theory of atomic structure, quantum electrodynamics (QED), in intense nuclear Coulomb fields. Tests of QED in many-electron ions are of particular interest since the spectra of high-Z many-electron ions are often more accessible experimentally than the spectra of the corresponding one-electron ions. To interpret these spectra, it is important to examine the level of accuracy with which one can understand ions with more than one electron. The system which is most intensively studied is the helium isoelectronic sequence.[2-4]

We wish to discuss here another multielectron system that is in some ways simpler, the lithium isoelectronic sequence. A particularly powerful calculational method for three-electron ions is many-body perturbation theory (MBPT), as recently demonstrated for neutral lithium by Lindgren.[5] In Ref. 5 it was shown that agreement with experiment at well under the 1% level could be obtained for the $2s$ and $2p$ spectra and hyperfine constants within the framework of nonrelativistic MBPT. Since neutral lithium is an essentially nonrelativistic system, tests of relativistic and QED effects are better made further out along the isoelectronic sequence. An attendant advantage of the study of an isoelectronic sequence is that the convergence of MBPT improves as Z increases, since the nuclear Coulomb field becomes increasingly dominant.

For systems in which relativistic and QED effects are enhanced, it is clearly important to have a formalism in which such effects are treated consistently. It has recently been shown[6] that a modification of the Furry representation of QED used by Mohr[4] in his work on the helium isoelectronic sequence provides a rigorous justification for the application of MBPT to relativistic many-electron systems. The modification consists of adding the core electron Hartree-Fock potential to the unperturbed Hamiltonian of QED and subtracting a corresponding counter term from the interaction Hamiltonian. The Breit interaction and the Lamb shift are contained naturally in the modified Furry formalism.

We find that the resulting version of MBPT gives a description of the lithium isoelectronic sequence that is accurate enough to isolate QED effects after one evaluates second- and third-order correlation energies, the Breit interaction, and the lowest-order correlation corrections to the Breit interaction. Indeed, we find that differences between theory and experiment for the $2p_{1/2}$-$2s_{1/2}$ energy intervals and for the $2p_{3/2}$-$2p_{1/2}$ fine structures are consistent with the one-electron Lamb shift. However, to account for these differences precisely an effective Z must be used in the one-electron Lamb-shift formulas, an effect referred to as screening of the Lamb shift. Since we are working in a framework based in QED, it is possible to identify Feynman graphs associated with this screening, and to describe the calculations necessary to account for it; this description will be given in Sec. IV.

The plan of the paper is as follows. In Sec. II the basic formulas are set up and expressions are given for the Breit interaction, the second- and third-order correlation energies, and the correlation corrections to the Breit interaction arising from diagrams containing one transverse photon and one Coulomb photon. The results of the calculation are presented for the lithium isoelectronic sequence in Sec. III along with some of the computational details. In Sec. IV comparison with experiment is made, and issues related to the screening of the Lamb shift are discussed.

II. FORMULAS

The starting point of our calculations is a frozen-core relativistic Hartree-Fock description of a three-electron

ion; the corresponding lowest-order contribution, $E^{(0)}$, to the energy of a valence electron is the Hartree-Fock eigenvalue, ε_v. The corrections to the lowest-order energy are treated using many-body perturbation theory (MBPT).

As discussed in Ref. 6, the formulas of MBPT can be shown to arise from a well-defined set of Feynman diagrams. The diagrams relevant to the present calculation are presented in Figs. 1–5. The crossed circle in some of the graphs represents a counterterm from the lowest-order potential, which in our case is the Hartree-Fock potential. Because we have chosen to work in Coulomb gauge, the photon propagator consists of two terms, a Coulomb interaction and a transverse interaction that reduces to the Breit interaction for low-Z ions.

Starting with Fig. 1, we note that the Coulomb part of the photon propagator leads to a contribution that exactly cancels the counterterm graphs (by the definition of the Hartree-Fock potential) so that only the exchange of a transverse photon need be considered. This photon can be exchanged between any pair of electrons, but since we are concerned with energy levels of the valence electron, only the terms involving the valence electron and either core electron need be considered. The associated first-order energy shift is

$$B^{(1)}=-\frac{\alpha}{2\pi^2}\sum_a \int d^3x\, d^3y \int d^3k\, e^{i\mathbf{k}\cdot(\mathbf{x}-\mathbf{y})}(\delta_{ij}-k_i k_j/|\mathbf{k}|^2) \times\left[\frac{1}{\mathbf{k}^2}\psi_v^\dagger(\mathbf{x})\alpha_i\psi_v(\mathbf{x})\psi_a^\dagger(\mathbf{y})\alpha_j\psi_a(\mathbf{y})-\frac{1}{\mathbf{k}^2-k_0^2}\psi_v^\dagger(\mathbf{x})\alpha_i\psi_a(\mathbf{x})\psi_a^\dagger(\mathbf{y})\alpha_j\psi_v(\mathbf{y})\right], \quad (1)$$

where $k_0=(1/c)|\varepsilon_v-\varepsilon_a|$. Methods for evaluating expressions involving matrix elements of $\boldsymbol{\alpha}$ between Dirac wave functions using vector spherical harmonics have been developed by Johnson and Mann;[7] some of the basic formulas are collected in Appendix A. The integration over $\mathbf{k}$ in the exchange part of Eq. (1) leads to a phase factor

$$e^{ik_0|\mathbf{x}-\mathbf{y}|}$$

that differs significantly from unity as one goes to high Z, and is therefore treated exactly; this requires evaluating the partial-wave expansion of the exchange term using spherical Bessel functions. The expression that is finally obtained is a generalization of the Breit interaction that correctly describes the exchange of a transverse photon in Coulomb gauge.

The remaining graphs involving only one-photon exchange are depicted in Fig. 2, and give the entire Lamb shift for a one-electron system. In the case of a many-electron system, there will be other effects of the same order arising from the graphs of Figs. 3–5 among others. Mohr[4] has shown for the two-electron problem that it is possible to assign an overall power of Z to each graph of the theory, though each graph involves an infinite power series in the parameter $Z\alpha$. The one-electron Lamb shift shown in Fig. 2 enters in order $Z^4\alpha^3$, with a factor $F(Z\alpha)$.[8] While, as mentioned above, Figs. 3 and 4 also contribute to order α^3, power-counting arguments show that they enter with one less power of Z. Therefore, as one goes along the isoelectronic sequence, inclusion of just the one-electron Lamb shift becomes an increasingly valid approximation.

In the treatment presented here, since we start from the Hartree-Fock potential instead of the nuclear Coulomb potential, the power-counting arguments cannot be carried through directly. However, the difference between the two potentials becomes small for large Z, so it can still be expected that the bulk of the Lamb shift will be accounted for by the one-electron formula

$$\Delta E_{nl_j}=\frac{\alpha^3Z^4}{\pi n^3}F_{nl_j}(Z\alpha)\ . \quad (2)$$

The functions $F(Z\alpha)$ for $n=2$ states are collected in Table II and the energy splittings that would arise from these terms are presented in Tables III and IV. These functions are taken from Ref. 8, with nuclear-finite-size corrections subtracted out, since finite-nuclear-size effects are included in the lowest-order Hartree-Fock calculation. It is important to stress that this is not an approach suited to systematically calculating screening corrections

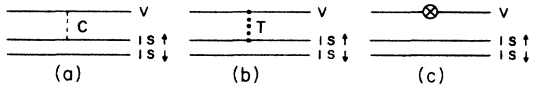

FIG. 1. Contributions to the first-order energy. The dashed line C in (a) represents a Coulomb photon, the dotted line T in (b) a transverse photon, and the crossed circle in (c) a Hartree-Fock counterterm. This type of diagram is summed over the two core electrons $1s\uparrow$ and $1s\downarrow$.

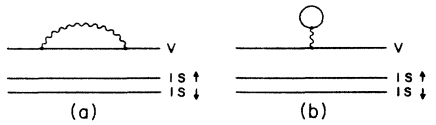

FIG. 2. First-order QED corrections to the energy. The valence electron self-energy (a) and vacuum-polarization (b) corrections. The wavy line represents a photon.

to the Lamb shift, but only a device to approximate an important physical contribution. A systematic QED approach to this problem will be outlined in Sec. IV.

Turning now to two-photon exchange, we first treat Fig. 4 in the case that the photons are both Coulomb photons. This problem has been examined recently both theoretically[6] and numerically[9] and is well understood; the formula for the corresponding second-order contribution to the correlation energy is

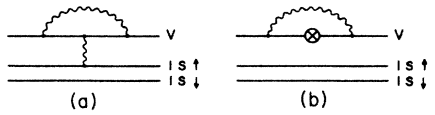

FIG. 3. A typical set of screening corrections to the valence electron self-energy.

$$E^{(2)}=-\sum_{a,m,n}\frac{g_{vamn}(g_{mnva}-g_{mnav})}{\varepsilon_m+\varepsilon_n-\varepsilon_v-\varepsilon_a}+\sum_{a,b,m}\frac{g_{abmv}(g_{mvab}-g_{mvba})}{\varepsilon_m+\varepsilon_v-\varepsilon_a-\varepsilon_b}$$
$$+\sum_{i(\neq v)}\frac{(V_{\rm HF}-U)_{vi}(V_{\rm HF}-U)_{iv}}{\varepsilon_v-\varepsilon_i}+\sum_{a,m}\left[\frac{(g_{vavn}-g_{vanv})(V_{\rm HF}-U)_{na}}{\varepsilon_a-\varepsilon_n}+\text{c.c.}\right],$$
$$(V_{\rm HF})_{ij}\equiv\sum_a(g_{iaja}-g_{iaaj})\ . \tag{3}$$

In Eq. (3) the quantities g_{ijkl} are two-electron Coulomb matrix elements. We adopt the convention that occupied core states are designated by subscripts $a,b,\ldots$, excited states are designated by $m,n,\ldots$, the valence state by v, and arbitrary states by $i,j,\ldots$. The quantity U is the potential used to define our basic states and $V_{\rm HF}$ is the core electron Hartree-Fock potential. Since we use $V_{\rm HF}$ to define our states the terms on the second line of Eq. (3) vanish. The angular decomposition of Eq. (3) is written out in Ref. 9 where a description is given of the methods used to carry out the sums over intermediate states n and m. Briefly, we introduce a finite basis set for the Dirac Hartree-Fock equations and replace the sums over the Hartree-Fock states in Eq. (3) by sums over the basis pseudospectrum.

We evaluate only the positive-energy intermediate-state contributions in Eq. (3). If one intermediate state occurs with negative energy and the other with positive energy, zero denominators could result; this is a phenomenon associated with continuum dissolution.[10] A full QED treatment excludes such terms, but allows a contribution where both propagators have negative energies, leading to a correction that is of the order of screening of the Lamb shift.

The next term treated in this calculation involves the graphs of Fig. 4, but with one or the other Coulomb photon replaced by a transverse photon. We treat such a term by generalizing the two-electron Coulomb matrix element that enters into the second-order energy formula, replacing g_{ijkl} in Eq. (3) by

$$g_{ijkl}\rightarrow g_{ijkl}+b_{ijkl}\ , \tag{4}$$

where b_{ijkl} is a two-electron matrix element of the Breit interaction, which is written out in detail in Appendix B. In our calculation of the one-Coulomb one-Breit terms we treat retardation only to lowest order, ignoring the phase discussed following Eq. (1). This is a reasonable approximation provided i, j, k, and l are all positive-energy states. However, a pitfall that arises from this approximation when negative-energy states are involved will now be discussed.

While we have accounted for the exchange of two Coulomb photons and of one Coulomb and one transverse photon, we have left out the exchange of two transverse photons. This is a correct procedure at the level of interest here, but care must be taken to distinguish between the Breit interaction and the exchange of a transverse photon to justify the procedure. It is well known[11] that treating the Breit operator to second order in conjunction with negative-energy states leads to a spuriously large contribution of the order of fine structure. This contribution arises from a term in which both intermediate electrons are in negative-energy states. While the associated denominator reduces the size of this term by α^2, the numerator is completely unsuppressed since the Breit interaction couples the large upper components of the wave function to the large lower components of the intermediate negative-energy states. We have directly evaluated such terms, and they do indeed enter in order $(Z\alpha)^2$ and spoil the relatively good agreement found with exper-

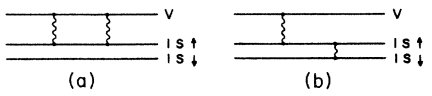

FIG. 4. Two typical second-order contributions to the valence energy.

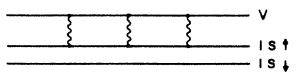

FIG. 5. A diagram contributing to the third-order valence energy.

iment. The resolution of this problem has to do with the phase factor discussed following Eq. (1). When a single transverse photon is exchanged, the phase factor is either strictly unity, for direct terms, or very close to unity, for exchange terms. Therefore, to a good approximation, one can evaluate the unretarded Breit interaction, making only a small error, and in this sense one can treat the Breit interaction as a term to be added to a many-body Hamiltonian. However, when the negative-energy state contribution is considered in second order, use of the Breit interaction is meaningless because the transverse photon exchange is accompanied by an extremely rapidly varying phase factor. The description in momentum space is that the photon propagator, $1/(\mathbf{k}^2-k_0^2)$, which normally is close to $1/\mathbf{k}^2$, behaves as $-1/4m^2$, a much smaller quantity due to the large energy transfer associated with exciting an electron-positron pair out of the vacuum. There is a nonvanishing contribution from this graph known to be important at the level of the Lamb shift[12] occurring in order $Z^3\alpha^3\ln(\alpha)$; this is one of the most important screening effects in the Lamb shift.

The next effect considered here is the exchange of three Coulomb photons; a sample graph is presented in Fig. 6. In this case we must evaluate the rather lengthy expression[13]

$$
\begin{aligned}
E^{(3)}=&\sum_{m,r,a,b,c}\frac{(g_{acrv}-g_{carv})(g_{vmba}-g_{mvba})(g_{rbmc}-g_{rbcm})}{(\varepsilon_v+\varepsilon_m-\varepsilon_a-\varepsilon_b)(\varepsilon_r+\varepsilon_v-\varepsilon_a-\varepsilon_c)}+\sum_{a,c,n,m,r}\frac{(g_{cvrm}-g_{vcrm})(g_{nmva}-g_{mnva})(g_{ranc}-g_{arnc})}{(\varepsilon_m+\varepsilon_n-\varepsilon_a-\varepsilon_v)(\varepsilon_r+\varepsilon_m-\varepsilon_c-\varepsilon_v)}\\
&+\sum_{n,m,a,b,c}\frac{(g_{camn}-g_{acmn})g_{nmba}(g_{vbvc}-g_{vbcv})}{(\varepsilon_n+\varepsilon_m-\varepsilon_a-\varepsilon_b)(\varepsilon_n+\varepsilon_m-\varepsilon_a-\varepsilon_c)}-\sum_{a,b,m,n,r}\frac{(g_{abrn}-g_{barn})g_{nmba}(g_{rvmv}-g_{vrmv})}{(\varepsilon_n+\varepsilon_m-\varepsilon_a-\varepsilon_b)(\varepsilon_r+\varepsilon_n-\varepsilon_a-\varepsilon_b)}\\
&+\sum_{n,a,b,c,d}\frac{(g_{cdvn}-g_{dcvn})g_{vnba}g_{badc}}{(\varepsilon_v+\varepsilon_n-\varepsilon_a-\varepsilon_b)(\varepsilon_v+\varepsilon_n-\varepsilon_c-\varepsilon_d)}+\sum_{a,n,m,r,s}\frac{(g_{avsr}-g_{vasr})g_{nmva}g_{rsnm}}{(\varepsilon_n+\varepsilon_m-\varepsilon_a-\varepsilon_v)(\varepsilon_r+\varepsilon_s-\varepsilon_a-\varepsilon_v)}\\
&+\left[\sum_{n,r,a,b,c}\frac{(g_{canr}-g_{acnr})(g_{nvba}-g_{nvab})(g_{rbvc}-g_{rbcv})}{(\varepsilon_n+\varepsilon_v-\varepsilon_a-\varepsilon_b)(\varepsilon_r+\varepsilon_n-\varepsilon_a-\varepsilon_c)}+\sum_{a,c,n,m,r}\frac{(g_{acrm}-g_{carm})(g_{nmva}-g_{mnva})(g_{rvnc}-g_{vrnc})}{(\varepsilon_m+\varepsilon_n-\varepsilon_a-\varepsilon_v)(\varepsilon_r+\varepsilon_m-\varepsilon_c-\varepsilon_a)}\right.\\
&\quad+\sum_{r,m,a,c,d}\frac{(g_{cdrm}-g_{dcrm})(g_{vmva}-g_{mvva})g_{radc}}{(\varepsilon_m-\varepsilon_a)(\varepsilon_r+\varepsilon_m-\varepsilon_c-\varepsilon_d)}+\sum_{m,r,s,a,c}\frac{(g_{acsr}-g_{casr})(g_{mvva}-g_{vmva})g_{rsmc}}{(\varepsilon_m-\varepsilon_a)(\varepsilon_r+\varepsilon_s-\varepsilon_c-\varepsilon_a)}\\
&\quad\left.+\sum_{a,b,s,m,r}\frac{(g_{absr}-g_{basr})g_{vmba}g_{rsmv}}{(\varepsilon_v+\varepsilon_m-\varepsilon_a-\varepsilon_b)(\varepsilon_r+\varepsilon_s-\varepsilon_a-\varepsilon_b)}+\sum_{n,m,a,c,d}\frac{(g_{cdmn}-g_{dcmn})g_{nmva}g_{vadc}}{(\varepsilon_n+\varepsilon_m-\varepsilon_a-\varepsilon_v)(\varepsilon_n+\varepsilon_m-\varepsilon_c-\varepsilon_d)}+\text{c.c.}\right].
\end{aligned}
\tag{5}
$$

To put this equation into a form suitable for numerical evaluation it is first necessary to carry out a somewhat involved angular momentum analysis. The details of this reduction to radial integrals are given in Appendix C. The numerical evaluation of the third-order energy was the most computationally intensive part of this work.

The final corrections considered here are those involving the finite mass of the nucleus. For the $2s$ states, we include only the effect of the reduced mass Rydberg, since mass polarization is known to be very small from symmetry considerations. For the $2p$ states we add the effect of mass polarization using the Hughes-Eckhart[14] formula,

$$\Delta E=-512\frac{m}{M}Z_1^5Z_2^5/(2Z_1+Z_2)^8\,,$$

$$Z_1=Z-0.3,\quad Z_2=Z-2\,. \tag{6}$$

The effect of the finite mass of the nucleus turns out to be small in comparison to the screening of the Lamb shift. For this reason the relatively crude treatment of mass polarization used here is sufficient; once Lamb-shift screening calculations are performed, a more rigorous and complete treatment of mass polarization will be needed.

III. TABULATION OF RESULTS

We now present the results of our calculations of the effects described in Sec. II. Table I contains a summary of all of the corrections described in Sec. II. In the

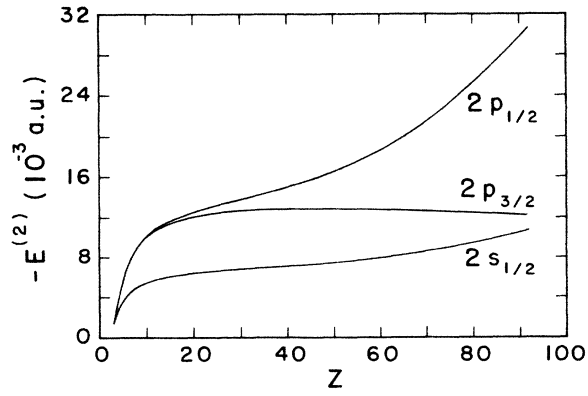

FIG. 6. The second-order Coulomb contribution to the valence electron energy $E^{(2)}$ plotted against nuclear charge Z for the three $n=2$ states of Li-like ions.

TABLE I. Contributions to the energies of $n=2$ states for Li-like ions. $s \equiv 2s_{1/2}$, $p^* \equiv 2p_{1/2}$, and $p \equiv 2p_{3/2}$.

	$E^{(0)}$	$E^{(2)}$	$E^{(3)}$	$B^{(1)}$	$B^{(2)}$	R.M.	Total
				$Z=3$			
s	−0.196 320	−0.001 649	−0.000 125(3)	0.000 005	−0.000 002	0.000 015	−0.198 076(3)
p^*	−0.128 638	−0.001 375	−0.000 145(3)	0.000 003	−0.000 001	0.000 008	−0.130 148(3)
p	−0.128 636	−0.001 374(1)	−0.000 145(3)	0.000 001	−0.000 001	0.000 008	−0.130 147(3)
				$Z=4$			
s	−0.666 183	−0.002 909	−0.000 159(5)	0.000 026	−0.000 008	0.000 041	−0.669 192(5)
p^*	−0.519 447	−0.003 962	−0.000 289(9)	0.000 027	−0.000 006	0.000 020	−0.523 657(9)
p	−0.519 406	−0.003 956(3)	−0.000 294(9)	0.000 013	−0.000 005	0.000 020	−0.523 628(9)
				$Z=5$			
s	−1.390 126	−0.003 719	−0.000 164(5)	0.000 069	−0.000 018	0.000 069	−1.393 889(5)
p^*	−1.167 352	−0.005 904	−0.000 335(10)	0.000 092	−0.000 016	0.000 033	−1.173 482(10)
p	−1.167 158	−0.005 891(4)	−0.000 341(10)	0.000 044	−0.000 015	0.000 033	−1.173 328(11)
				$Z=6$			
s	−2.365 898	−0.004 276	−0.000 161(6)	0.000 143	−0.000 030	0.000 108	−2.370 114(6)
p^*	−2.068 823	−0.007 278	−0.000 341(12)	0.000 215	−0.000 031	0.000 049	−2.076 209(12)
p	−2.068 242	−0.007 254(5)	−0.000 347(12)	0.000 101	−0.000 028	0.000 049	−2.075 721(13)
				$Z=7$			
s	−3.592 973	−0.004 681	−0.000 154(6)	0.000 255	−0.000 046	0.000 141	−3.597 458(6)
p^*	−3.222 506	−0.008 280(1)	−0.000 330(12)	0.000 410	−0.000 051	0.000 062	−3.230 695(12)
p	−3.221 143	−0.008 244(5)	−0.000 336(12)	0.000 192	−0.000 046	0.000 062	−3.229 515(13)
				$Z=8$			
s	−5.071 312	−0.004 988	−0.000 146(6)	0.000 414	−0.000 065	0.000 174	−5.075 923(6)
p^*	−4.627 921	−0.009 039(1)	−0.000 313(12)	0.000 696	−0.000 076	0.000 075	−4.636 578(12)
p	−4.625 184	−0.008 989(6)	−0.000 318(12)	0.000 325	−0.000 068	0.000 075	−4.634 159(13)
				$Z=9$			
s	−6.801 084	−0.005 229	−0.000 136(5)	0.000 628	−0.000 087	0.000 196	−6.805 712(5)
p^*	−6.284 988	−0.009 635(1)	−0.000 296(12)	0.001 087	−0.000 105	0.000 083	−6.293 854(12)
p	−6.280 043	−0.009 567(6)	−0.000 301(12)	0.000 506	−0.000 094(1)	0.000 083	−6.289 416(12)
				$Z=10$			
s	−8.782 576	−0.005 424	−0.000 127(5)	0.000 904	−0.000 111	0.000 241	−8.787 093(5)
p^*	−8.193 839	−0.010 117(1)	−0.000 277(10)	0.001 601	−0.000 139	0.000 100	−8.202 671(10)
p	−8.185 571	−0.010 029(6)	−0.000 281(10)	0.000 743	−0.000 124(1)	0.000 100	−8.195 162(12)
				$Z=11$			
s	−11.016 162	−0.005 585	−0.000 119(5)	0.001 250	−0.000 139	0.000 263	−11.020 492(5)
p^*	−10.354 738	−0.010 516(1)	−0.000 262(10)	0.002 254	−0.000 177	0.000 108	−10.363 331(10)
p	−10.341 711	−0.010 405(6)	−0.000 266(10)	0.001 044	−0.000 159(1)	0.000 108	−10.351 389(12)
				$Z=13$			
s	−16.241 446	−0.005 836	−0.000 107(5)	0.002 187	−0.000 203	0.000 330	−16.245 075(5)
p^*	−15.434 218	−0.011 144(1)	−0.000 234(12)	0.004 044	−0.000 269	0.000 134	−15.441 687(12)
p	−15.405 867	−0.010 979(7)	−0.000 238(12)	0.001 865	−0.000 239(1)	0.000 133	−15.415 325(14)
				$Z=15$			
s	−22.481 209	−0.006 024	−0.000 097(5)	0.003 504	−0.000 278	0.000 398	−22.483 706(5)
p^*	−21.527 233	−0.011 623(1)	−0.000 213(11)	0.006 591	−0.000 379	0.000 160	−21.532 697(11)
p	−21.472 903	−0.011 394(7)	−0.000 215(11)	0.003 026	−0.000 336(2)	0.000 159	−21.481 663(13)
				$Z=17$			
s	−29.740 649	−0.006 172	−0.000 088(5)	0.005 267	−0.000 363	0.000 466	−29.741 539(5)
p^*	−28.638 629	−0.012 011(1)	−0.000 193(10)	0.010 030	−0.000 509	0.000 186	−28.641 126(10)
p	−28.543 569	−0.011 706(7)	−0.000 194(10)	0.004 584	−0.000 448(2)	0.000 185	−28.551 148(12)

TABLE I. (*Continued*).

	$E^{(0)}$	$E^{(2)}$	$E^{(3)}$	$B^{(1)}$	$B^{(2)}$	R.M.	Total
				$Z=20$			
s	−42.555 295	−0.006 347	−0.000 079(4)	0.008 895	−0.000 509	0.000 584	−42.552 751(4)
p^*	−41.228 125	−0.012 489(1)	−0.000 171(9)	0.017 162	−0.000 740	0.000 231	−41.224 132(9)
p	−41.033 621	−0.012 048(7)	−0.000 172(9)	0.007 788	−0.000 645(3)	0.000 229	−41.038 469(12)
				$Z=22$			
s	−52.392 598	−0.006 443	−0.000 075(4)	0.012 069	−0.000 620	0.000 599	−52.387 068(4)
p^*	−50.912 869	−0.012 764(1)	−0.000 161(8)	0.023 437	−0.000 919	0.000 237	−50.903 039(8)
p	−50.618 187	−0.012 219(7)	−0.000 158(8)	0.010 581	−0.000 795(3)	0.000 233	−50.620 545(11)
				$Z=24$			
s	−63.274 938	−0.006 528	−0.000 069(5)	0.015 930	−0.000 739	0.000 668	−63.265 676(5)
p^*	−61.640 358	−0.013 019(1)	−0.000 151(10)	0.031 095	−0.001 119(1)	0.000 264	−61.623 288(10)
p	−61.210 751	−0.012 357(7)	−0.000 148(10)	0.013 963	−0.000 960(3)	0.000 259	−61.209 994(13)
				$Z=26$			
s	−75.211 664	−0.006 605	−0.000 065(5)	0.020 549	−0.000 868	0.000 737	−75.197 916(5)
p^*	−73.419 685	−0.013 260(1)	−0.000 142(10)	0.040 284	−0.001 340(1)	0.000 291	−73.393 852(10)
p	−72.812 977	−0.012 470(7)	−0.000 139(10)	0.017 983	−0.001 140(4)	0.000 285	−72.808 458(13)
				$Z=28$			
s	−88.213 154	−0.006 677	−0.000 061(3)	0.026 000	−0.001 007	0.000 834	−88.194 065(3)
p^*	−86.260 934	−0.013 493(1)	−0.000 132(7)	0.051 152	−0.001 583(1)	0.000 329	−86.224 661(7)
p	−85.426 702	−0.012 562(7)	−0.000 130(7)	0.022 693	−0.001 333(4)	0.000 321	−85.417 713(11)
				$Z=30$			
s	−102.290 766	−0.006 745	−0.000 058(4)	0.032 359	−0.001 154(1)	0.000 877	−102.265 487(4)
p^*	−100.175 218	−0.013 723(1)	−0.000 126(8)	0.063 855	−0.001 848(1)	0.000 346	−100.126 714(8)
p	−99.053 935	−0.012 638(7)	−0.000 124(8)	0.028 139	−0.001 540(5)	0.000 336	−99.039 762(12)
				$Z=33$			
s	−125.452 560	−0.006 842	−0.000 054(3)	0.043 769	−0.001 393(1)	0.000 918	−125.416 162(3)
p^*	−123.085 530	−0.014 067(1)	−0.000 117(6)	0.086 696	−0.002 290(1)	0.000 363	−123.014 945(6)
p	−121.399 933	−0.012 727(7)	−0.000 114(6)	0.037 792	−0.001 876(5)	0.000 351	−121.376 507(10)
				$Z=36$			
s	−151.110 904	−0.006 933(4)	−0.000 050(4)	0.057 669	−0.001 649(4)	0.000 987	−151.060 880(7)
p^*	−148.483 703	−0.014 410(8)	−0.000 109(8)	0.114 575	−0.002 777(7)	0.000 391	−148.386 033(13)
p	−146.039 376	−0.012 780(6)	−0.000 106(8)	0.049 354	−0.002 238(3)	0.000 375	−146.004 771(10)
				$Z=41$			
s	−199.569 770	−0.007 094(4)	−0.000 046(2)	0.087 154	−0.002 131(4)	0.001 177	−199.490 710(6)
p^*	−196.486 550	−0.015 032(9)	−0.000 101(5)	0.173 837	−0.003 737(8)	0.000 470	−196.331 113(13)
p	−192.226 485	−0.012 851(6)	−0.000 095(5)	0.073 230	−0.002 908(4)	0.000 445	−192.168 664(9)
				$Z=54$			
s	−360.954 305	−0.007 581(5)	−0.000 038(2)	0.210 629	−0.003 713(7)	0.001 500	−360.753 508(9)
p^*	−356.517 745	−0.017 014(10)	−0.000 086(4)	0.422 942	−0.007 164(13)	0.000 615	−356.118 452(17)
p	−342.606 186	−0.012 886(7)	−0.000 075(4)	0.165 488	−0.004 974(5)	0.000 557	−342.458 076(10)
				$Z=74$			
s	−724.786 626	−0.008 750(6)	−0.000 033(2)	0.597 201	−0.007 463(5)	0.002 161	−724.203 510(8)
p^*	−717.568 648	−0.021 963(14)	−0.000 078(4)	1.209 050	−0.016 294(11)	0.000 943	−716.396 990(18)
p	−661.623 891	−0.012 664(8)	−0.000 058(2)	0.399 627	−0.008 829(3)	0.000 776	−661.245 039(9)
				$Z=92$			
s	−1209.744 297	−0.010 720(10)	−0.000 032(2)	1.287 925	−0.013 489(18)	0.002 788	−1208.477 83(2)
p^*	−1199.179 877	−0.030 672(19)	−0.000 081(4)	2.638 944	−0.032 206(35)	0.001 317	−1196.602 58(4)
p	−1043.794 272	−0.012 246(10)	−0.000 048(2)	0.690 718	−0.012 616(11)	0.000 959	−1043.127 51(2)

second column of Table I, we present the Hartree-Fock energies $E^{(0)}$ for the states of interest here, $2s_{1/2}$, $2p_{1/2}$, and $2p_{3/2}$. The third column of the table gives the second-order energy $E^{(2)}$ calculated from Eq. (3). This quantity is necessarily approximate, owing to the finite size of the basis set and the need to truncate the partial-wave expansions. The error from the former is small since we use a large basis set involving 40 positive-energy states. To estimate the error from the latter, the partial-wave expansion was extended from $l=0$ through 8. After the $l=2$ term, a smooth pattern of convergence was observed. The error quoted is the difference between successive Aitken's extrapolations using $l=3$, 4, 5, 6, and 7, and $l=4$, 5, 6, 7, and 8. This error could be reduced by including more partial waves.

We plot in Fig. 6 the second-order energies of the three $n=2$ states along the lithium isoelectronic sequence. In the nonrelativistic $1/Z$ approximation these energies are constants. The clearly nonconstant behavior of our calculated results comes from two effects. The differences at low Z arise because we evaluate $E^{(2)}$ in a Hartree-Fock potential, which is significantly different from the Coulomb potential. For larger Z, however, the two potentials are similar and the deviation from constancy, which is particularly pronounced for the $j=\frac{1}{2}$ states, is a relativistic effect reflecting the fact that the coefficient of the Z^0 term in the $1/Z$ expansion is a function of $Z\alpha$, analogous to the function $F(Z\alpha)$ in Eq. (2).

As mentioned in Sec. II, the third-order energy $E^{(3)}$, given in the fourth column of Table I, was much more computationally demanding, and is therefore less accurately known. The most time-consuming term to evaluate was the sixth term in Eq. (5). This term involves a quadruple sum over excited states. While any one angular momentum channel in this term can be evaluated in a few seconds on a CRAY X-MP/48, as higher l values in the partial-wave expansions of the Coulomb integrals are included, the number of channels increases very rapidly. By using a relatively small basis set of 20 positive-energy functions we were able to sum terms up to $l=4$ in about 5 min per state. The error estimates for the third-order energy given in Table I, which range from 3% to 5%, are conservative, and could easily be reduced to under 1% with sufficient computer time, about 45 min per state. Because the third-order energy is significantly smaller than the second-order energy, our conclusions are not affected by the relatively large error. A plot of $E^{(3)}$ along the isoelectronic sequence is shown in Fig. 7. In a $1/Z$ expansion, $E^{(3)}$ decreases as $1/Z$; the deviations from this $1/Z$ behavior in Fig. 7 have the same origins as the deviations discussed in connection with Fig. 6.

The fifth column of Table I gives the contributions of the first-order transverse interaction $B^{(1)}$ derived from Eq. (1), with retardation included exactly. In Fig. 8 we plot $B^{(1)}/Z^3$ (in solid lines) together with the usual Breit interaction (in dashed lines); in a $1/Z$ expansion the Breit interaction is expected to be proportional to Z^3. The sixth column of Table I gives the effect of terms linear in b_{ijkl} in the second-order energy $B^{(2)}$. This term also involves a partial-wave-expansion, and its error is evaluated in the same manner as described above for the second-

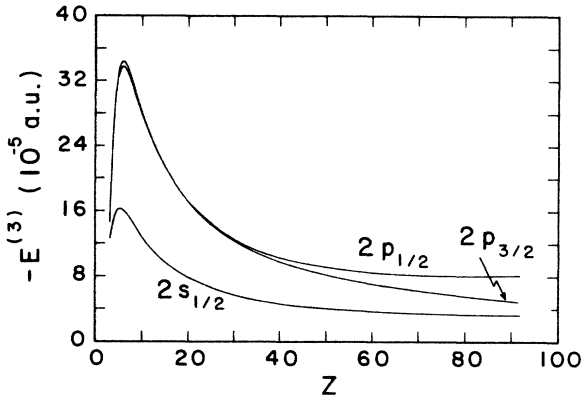

FIG. 7. The third-order Coulomb contribution to the valence electron energy $E^{(3)}$ plotted against nuclear charge Z.

order Coulomb energy. A plot of $B^{(2)}$ is presented in Fig. 9. In the nonrelativistic $1/Z$ approximation this term is proportional to Z^2; deviations from this behavior occur for the reasons discussed above. Next, in the column labeled R.M., the combination of the Hughes-Eckart formula, Eq. (6), together with the correction from the reduced mass Rydberg is given. The final column in Table I gives the sum of all of the preceding terms.

All of the calculations described above were done assuming a Fermi distribution for the nuclear charge. The thickness parameter in the Fermi distribution was taken to be $t_{\rm nuc}=2.3$ fm.; the corresponding 50% density radius, $c_{\rm nuc}$, is listed in Table II for the ions considered in Table I. Also given in Table II are values of the functions $F(Z\alpha)$ for the $n=2$ states of one-electron atoms that are used in Tables III and IV.

While valence energies can be accurately measured for low values of Z, better data exist along the isoelectronic sequence for the energy differences. In Tables III and IV we compare our results for energy differences with experiment. We use experimental data compiled by Edlén and supplemented by recent measurements by Denne and Hinnov.[15] Our results for the $2s_{1/2}$-$2p_{1/2}$ energy inter-

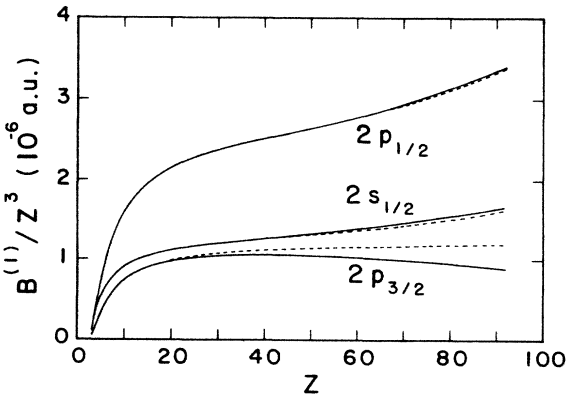

FIG. 8. The first-order transverse photon contribution to the valence electron energy $B^{(1)}$ plotted against nuclear charge Z.

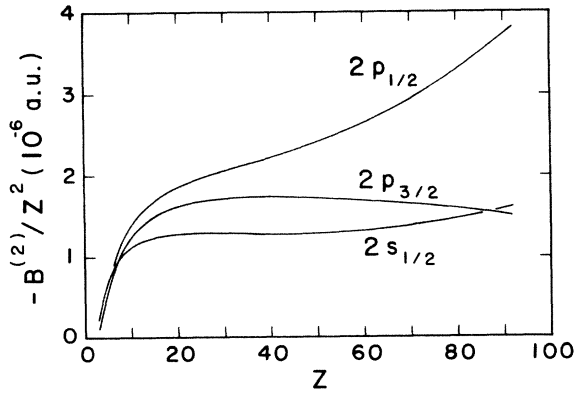

FIG. 9. The second-order transverse photon contribution to the valence electron energy $B^{(2)}$ plotted against nuclear charge Z.

vals are presented in Table III and results for the $2p$ fine-structure splittings are given in Table IV. Since we have not included the QED corrections, we compare the difference between our theoretical values and experiment to the one-electron Lamb shift given in Eq. (2). From these comparisons one can see that the bulk of the difference is indeed accounted for by Eq. (2) but that systematic discrepancies remain. Because of the pattern of convergence shown in Table I it is clear that the

TABLE II. Nuclear charge distribution parameters $c_{\rm nuc}$ and Coulomb field Lamb-shift values $F_{nl_j}(Z\alpha)$ for Li-like ions.

Z	A	$c_{\rm nuc}$	$F_{2s_{1/2}}$	$F_{2p_{1/2}}$	$F_{2p_{3/2}}$
3	7	1.800	7.4759	−0.1247	0.1241
4	9	2.067	6.7674	−0.1238	0.1247
5	11	1.810	6.2284	−0.1225	0.1254
6	12	1.935	5.7981	−0.1211	0.1261
7	14	2.127	5.4409	−0.1197	0.1270
8	16	2.438	5.1375	−0.1181	0.1279
9	19	2.777	4.8752	−0.1164	0.1289
10	20	2.989	4.6451	−0.1146	0.1300
11	23	2.885	4.4409	−0.1128	0.1311
13	27	3.017	4.0931	−0.1089	0.1335
15	31	3.275	3.8062	−0.1047	0.1360
17	35	3.497	3.5645	−0.1004	0.1388
20	40	3.719	3.2650	−0.0934	0.1431
22	48	3.275	3.0971	−0.0884	0.1462
24	52	3.929	2.9494	−0.0834	0.1494
26	56	4.118	2.8183	−0.0781	0.1528
28	58	4.178	2.7013	−0.0727	0.1561
30	64	4.445	2.5962	−0.0672	0.1597
33	75	4.665	2.4576	−0.0554	0.1651
36	84	4.849	2.3381	−0.0494	0.1707
41	93	4.977	2.1728	−0.0336	0.1803
54	132	5.702	1.8821	0.0126	0.2068
74	184	6.446	1.6738	0.1041	0.2506
92	238	6.987	1.6436	0.2240	0.2916

TABLE III. Differences between theory and experiment for the $2p_{1/2}$-$2s_{1/2}$ energy interval (a.u.) in Li-like ions are compared with one-electron Lamb-shift calculations.

Z	Theory[a]	Experiment[b]	Difference	Negative Lamb shift[c]
3	0.067 928(4)	0.067 906	0.000 022(4)	0.000 010
4	0.145 54(1)	0.145 48	0.000 06(1)	0.000 03
5	0.220 41(1)	0.220 34	0.000 07(1)	0.000 06
6	0.293 91(1)	0.293 81	0.000 10(1)	0.000 12
7	0.366 76(1)	0.366 62	0.000 14(1)	0.000 21
8	0.439 34(1)	0.439 12	0.000 22(1)	0.000 33
9	0.511 86(1)	0.511 50(1)	0.000 36(2)	0.000 51
10	0.584 42(1)	0.583 90(1)	0.000 52(1)	0.000 74
11	0.657 16(1)	0.656 40(1)	0.000 76(2)	0.001 03
13	0.803 39(1)	0.801 97(2)	0.001 42(2)	0.001 86
15	0.951 01(1)	0.948 49(5)	0.002 52(6)	0.003 06
17	1.100 41(1)	1.096 52(5)	0.003 89(6)	0.004 73
20	1.328 62(1)	1.321 56(4)	0.007 06(4)	0.008 31
22	1.484 03(1)	1.474 20(4)	0.009 83(4)	0.011 54
24	1.642 39(1)	1.6290(1)	0.0134(1)	0.015 56
26	1.804 06(1)	1.7861(1)	0.0180(1)	0.020 46
28	1.969 40(1)	1.9460(4)	0.0234(4)	0.026 36
30	2.138 77(1)			0.033 36
33	2.401 22(1)			0.046 08
36	2.674 85(1)	2.6181(4)	0.0568(4)	0.062 00
41	3.159 60(1)			0.096 40
54	4.635 06(2)			0.2458
74	7.806 52(2)			0.7278
92	11.875 25(5)			1.5724

[a]Numbers in parentheses give the error in the last digit.
[b]Reference 15.
[c]Reference 8.

TABLE IV. Differences between experiment and theory for the $2p_{3/2}$-$2p_{1/2}$ fine-structure interval (a.u.) in Li-like ions are compared with the one-electron Lamb shift.

Z	Theory[a]	Experiment[b]	Difference	Lamb shift[c]
3	0.000 002(4)	0.000 002	0.000 000(4)	0.000 000
4	0.000 03(1)	0.000 03	0.000 00(1)	0.000 00
5	0.000 15(1)	0.000 16	0.000 01(2)	0.000 00
6	0.000 49(2)	0.000 49	0.000 00(2)	0.000 01
7	0.001 18(2)	0.001 18	0.000 00(2)	0.000 01
8	0.002 42(2)	0.002 42	0.000 00(2)	0.000 02
9	0.004 44(2)	0.004 45(1)	0.000 01(2)	0.000 02
10	0.007 51(2)	0.007 51(1)	0.000 00(2)	0.000 04
11	0.011 94(2)	0.011 99(2)	0.000 05(3)	0.000 06
13	0.026 36(2)	0.026 41(2)	0.000 05(3)	0.000 11
15	0.051 03(2)	0.051 27(7)	0.000 24(7)	0.000 19
17	0.089 98(2)	0.090 08(7)	0.000 10(7)	0.000 31
20	0.185 66(1)	0.186 13(4)	0.000 47(5)	0.000 59
22	0.282 49(1)	0.283 16(4)	0.000 67(4)	0.000 85
24	0.413 29(2)	0.4142(1)	0.0009(1)	0.001 19
26	0.585 39(2)	0.5867(1)	0.0013(1)	0.001 63
28	0.806 95(1)	0.8088(9)	0.0018(9)	0.002 17
30	1.086 95(1)			0.002 84
33	1.638 44(1)			0.004 04
36	2.381 26(2)	2.3855(12)	0.0042(12)	0.005 72
41	4.162 45(2)			0.009 35
54	13.660 38(2)			0.025 53
74	55.151 95(2)			0.067 92
92	153.475 07(4)			0.074 88

[a]Numbers in parentheses give the error in the last digit.

discrepancies cannot be accounted for by atomic structure uncertainties, but instead are QED effects, which we now discuss.

IV. INTERPRETATION IN TERMS OF QED EFFECTS

Comparison of theory and experiment for the $2s_{1/2}$-$2p_{1/2}$ splitting and fine structure clearly shows an effect that is of the order of the one-electron Lamb shift, but that is systematically smaller. Both Grant[16] and Desclaux[17] account for the Lamb shift in their Hartree-Fock codes by replacing Z by a slightly reduced value Z' in the one-electron formula, Eq. (2). However, there is necessarily some arbitrariness in the procedure for choosing Z', and any remaining discrepancy with theory could be attributed to the choice of Z' even if a real breakdown of QED were present. A more fundamental approach to the problem is to evaluate the contributions from QED that have not yet been considered. These are associated with the Feynman graphs of Figs. 2, 3, and 4, which we discuss in turn.

The self-energy and vacuum-polarization graphs of Fig. 2 have been extensively treated in the case of a Coulomb field. One possible approach that would eliminate the need for further discussion of these terms would be to reformulate the entire calculation described in Sec. II using a nuclear Coulomb potential instead of the Hartree-Fock potential; then the results of Ref. 8 could be taken over directly. However, in that case the present calculation would have to be redone using a Coulomb potential, and a significantly larger number of graphs would have to be computed. Since the extra graphs generally require significantly less computer time to evaluate, we consider this an attractive possibility. An attendant advantage of dealing with the local Coulomb potential is that the simpler Feynman gauge is known to give results identical to those that arise from the rather complex Coulomb gauge expressions.

If the Hartree-Fock potential is used, the graphs of Fig. 2 must be evaluated in that potential for a theoretically consistent calculation. This means that the entire Lamb-shift calculation must be redone. While this is a large-scale effort, a similar calculation has been carried out by Desiderio and Johnson[18] for the case of a local Hartree-Fock-Slater potential. We are presently investigating the question of whether the use of the same finite basis set techniques as used to evaluate $E^{(2)}$, $E^{(3)}$, and $B^{(2)}$ can facilitate a Lamb-shift calculation for the Hartree-Fock potential.

The next calculation that would need to be performed is the complete evaluation of the box graphs of Fig. 4. We have, of course, evaluated the dominant parts of these graphs already by computing $E^{(2)}$ and $B^{(2)}$. However, there are extra terms that will contribute to the screening of the Lamb shift. As discussed in Ref. 6, Eq. (3) can be derived from the full QED expression corresponding to Fig. 4 only after a contour integration has been performed. Along with positive-energy terms, terms in which both electrons have negative energy arise, and these terms have not been included in our analysis. They are, however, entirely trivial to evaluate, involving only a rearrangement of the sums over intermediate states in

our computer codes. A less trivial effect arises from the pole structure of transverse photons. While Coulomb photons have no pole structure, the contour integration will include photon poles when one or two transverse photons are present, and these will lead to a new kind of structure in which a photon energy integration is present in addition to the sums over intermediate electron states. These new terms could either be directly evaluated, or as an alternative the contour integration could be done differently. It is possible to rotate the contour of integration parallel to the imaginary axis, being careful to avoid poles and cuts in the complex plane, instead of encircling poles and eliminating an integration via Cauchy's theorem. This method was used by Lakdawala and Mohr[19] in similar work on the hyperfine structure of muonic helium. Even more so than with the Lamb shift it seems likely that finite basis set techniques will simplify the complete evaluation of Fig. 4.

The last contribution that we expect to be important at the level of the Lamb-shift screening comes from the graphs of Fig. 3. While these graphs have ultraviolet divergences, they are somewhat simpler than those of the Lamb shift, and cancel with other graphs of the same class because of the Ward identity. Mohr[20] has recently presented formulas for these terms for helium. While complicated to work out exactly, it may be an accurate approximation to replace the vertex and self-energy terms by their free-space values, which in Coulomb gauge have recently been presented by Adkins.[21] Once again, finite basis set techniques may prove valuable in the complete evaluation of these terms.

While a great deal of work clearly remains to be done to understand the spectra of the $n=2$ terms along the lithium isoelectronic sequence at the level of experimental uncertainty, the point that we wish to stress is that the remaining uncalculated terms are all QED effects. These effects are particularly interesting aspects of QED because they test not only the interaction of an electron with the radiation field, but also the interaction of an electron with the radiation field in the presence of other electrons. If indeed QED is the underlying theory of many-electron as well as one-electron atoms, such effects should be calculable and agree with experiment. However, before QED can be tested, it is important to be sure that one has control of traditional atomic structure effects. We believe that, by including the terms calculated in this paper, these effects are uncertain by much less than the screening of the Lamb shift. This is based on the behavior shown in Table I: the Hartree-Fock energy grows roughly as Z^2, the second-order energy is roughly constant, and the third-order energy falls for high Z roughly as $1/Z$. We can also examine a subset of fourth-order corrections formed by "chaining" two second-order energies, that is, by replacing the valence states v occurring in the ket position in $E^{(2)}$ by their Brueckner orbital corrections. On energy denominator grounds, this is likely to be a numerically important subset of the total fourth-order energy. At $Z=28$, for example, the resulting fourth-order corrections to the $2s$ state are only -5.6×10^{-7}, 0.002% of the $2s$ Lamb shift. Similarly, the first-order Coulomb corrections to the Breit interaction is smaller than the lowest-order Breit interaction by a factor of Z so that further corrections should again be entirely negligible at the level of interest. Of course, for smaller values of Z, the full complexity of the many-body problem comes into play, and higher-order terms must be considered. Even at $Z=3$, however we have found that after including the subset of fourth-order terms mentioned above, the removal energies for the three states agree with calculation at the few ppm level, so that even for low Z going to the next order of MBPT may reduce atomic structure uncertainties to the level of QED effects.

In summary, the $n=2$ states along the lithium isoelectronic sequence have been treated in the framework of MBPT. By going to third order in the Coulomb interaction and second order in the Breit plus Coulomb interaction, the most important non-QED atomic structure contributions have been included. Comparison with experiment shows systematic deviations from the one-electron Lamb shift, illustrating the need for a full QED calculation of this radiative correction in a many-electron atom. The relevant diagrams have been identified and discussed. It is our feeling that because of this, precision studies of the spectrum of the lithium isoelectronic sequence are of fundamental importance, on par with the studies that have been made of the helium isoelectronic sequence. Completion of the screening calculations listed above, together with accurate experiments for high values of Z, will not only test QED in intense nuclear Coulomb fields, but will also test our understanding of the relativistic atomic many-body problem.

ACKNOWLEDGMENTS

The authors would like to thank H. G. Berry, H. Gould, A. E. Livingston, P. Mohr, and D. Yennie for valuable discussions and encouragement. This work was supported in part by National Science Foundation Grants No. PHY-85-03415 and No. PHY-86-08101.

APPENDIX A: VECTOR SPHERICAL HARMONICS

Evaluation of Coulomb integrals with Dirac wave functions leads to the basic angular integral

$$I_{JM}(\kappa_b m_b,\kappa_a m_a) \equiv \int d\Omega \chi^{\dagger}_{\kappa_b m_b}(\theta,\phi) Y_{JM}(\theta,\phi) \chi_{\kappa_a m_a}(\theta,\phi) , \tag{A1}$$

where the solution of the Dirac equation is taken to be

$$\psi_{\kappa m}(\mathbf{r}) = \frac{1}{r} \begin{bmatrix} ig(r) & \chi_{\kappa m}(\theta,\phi) \\ f(r) & \chi_{-\kappa m}(\theta,\phi) \end{bmatrix} . \tag{A2}$$

The spherical spinors χ are defined as

$$\chi_{\kappa m}(\theta,\phi) \equiv \begin{bmatrix} 1 \\ 0 \end{bmatrix} Y_{l\, m-1/2}(\theta,\phi) \langle lm, \tfrac{1}{2}\tfrac{1}{2} \mid jm \rangle + \begin{bmatrix} 0 \\ 1 \end{bmatrix} Y_{l\, m+1/2} \langle lm, \tfrac{1}{2} -\tfrac{1}{2} \mid jm \rangle , \tag{A3}$$

where if $j=l+\frac{1}{2}$, $\kappa=-1-l$, and if $j=l-\frac{1}{2}$, $\kappa=l$. These obey the basic rules

$$\sigma_r\chi_{\kappa m}(\theta,\phi)=-\chi_{-\kappa m}(\theta,\phi)\ , \tag{A4a}$$

$$\boldsymbol{\sigma}\cdot\mathbf{L}\chi_{\kappa m}(\theta,\phi)=-(1+\kappa)\chi_{\kappa m}(\theta,\phi)\ , \tag{A4b}$$

$$i\boldsymbol{\sigma}\cdot(\hat{\mathbf{r}}\times\mathbf{L})\chi_{\kappa m}(\theta,\phi)=(1+\kappa)\chi_{-\kappa m}(\theta,\phi)\ . \tag{A4c}$$

The integral I_{JM} in Eq. (A1) is related to the reduced matrix element of the normalized spherical harmonics $C_{JM}\equiv\sqrt{4\pi/(2J+1)}Y_{JM}$ by

$$I_{JM}=\sqrt{(2J+1)/4\pi}(-1)^{j_b-m_b}\begin{pmatrix} j_b & J & j_a \\ -m_b & M & m_a\end{pmatrix}\times\langle\kappa_b\|C_J\|\kappa_a\rangle\ , \tag{A5}$$

where

$$\langle\kappa_b\|C_J\|\kappa_a\rangle\equiv C_J(ba)=(-1)^{[J_b+(1/2)]}\sqrt{[a][b]}\begin{pmatrix} j_a & J & j_b \\ \frac{1}{2} & 0 & -\frac{1}{2}\end{pmatrix}\times\Pi(l_a,l_b,J)\ ,$$

$$\Pi(l_a,l_b,J)=\begin{cases}1 & \text{if } l_a+l_b+J \text{ is even}\\ 0 & \text{if } l_a+l_b+J \text{ is odd}\end{cases}\ . \tag{A6}$$

When considering the Breit interaction one encounters the expression

$$\chi^\dagger_{\kappa_b m_b}(\theta,\phi)\boldsymbol{\sigma}\chi_{\kappa_a m_a}(\theta,\phi)\ . \tag{A7}$$

In order to deal with such structures, we introduce vector spherical harmonics, which are defined in a manner analogous to spherical spinors,

$$\mathbf{Y}_{JLM}(\theta,\phi)\equiv\sum_{m,q}Y_{Lm}(\theta,\phi)\mathbf{e}_q\langle Lm,1q\,|\,JM\rangle\ , \tag{A8}$$

where $\mathbf{e}_0\equiv\hat{\mathbf{z}}$, $\mathbf{e}_1\equiv-\sqrt{\frac{1}{2}}(\hat{\mathbf{x}}+i\hat{\mathbf{y}})$, and $\mathbf{e}_{-1}\equiv\sqrt{\frac{1}{2}}(\hat{\mathbf{x}}-i\hat{\mathbf{y}})$. It is straightforward to show that these quantities are related to the following basic vector operations on the spherical harmonics:

$$\frac{\mathbf{L}}{\sqrt{J(J+1)}}Y_{JM}=\mathbf{Y}_{JJM}\ , \tag{A9a}$$

$$\hat{\mathbf{r}}Y_{JM}=-\left[\frac{J+1}{2J+1}\right]^{1/2}\mathbf{Y}_{JJ+1M}+\left[\frac{J}{2J+1}\right]^{1/2}\mathbf{Y}_{JJ-1M}\ , \tag{A9b}$$

$$\frac{r\boldsymbol{\nabla}}{\sqrt{J(J+1)}}Y_{JM}=\left[\frac{J}{2J+1}\right]^{1/2}\mathbf{Y}_{JJ+1M}+\left[\frac{J+1}{2J+1}\right]^{1/2}\mathbf{Y}_{JJ-1M}\ . \tag{A9c}$$

Since the vector spherical harmonics obey the orthogonality condition

$$\int d\Omega\mathbf{Y}^\dagger_{JLM}(\theta,\phi)\cdot\mathbf{Y}_{J'L'M'}(\theta,\phi)=\delta_{JJ'}\delta_{LL'}\delta_{MM'}\ , \tag{A10}$$

if we expand Eq. (A7) as

$$\chi^\dagger_{\kappa_b m_b}(\theta,\phi)\boldsymbol{\sigma}\chi_{\kappa_a m_a}(\theta,\phi)\equiv\sum_{J,L,M}C_{JLM}(\kappa_b m_b,\kappa_a m_a)\mathbf{Y}_{JLM}(\theta,\phi)\ , \tag{A11}$$

then the coefficients C_{JLM} can be written as

$$C_{JLM}(\kappa_b m_b,\kappa_a m_a)=\langle\kappa_b m_b\,|\,\mathbf{Y}^\dagger_{JLM}\cdot\boldsymbol{\sigma}\,|\,\kappa_a m_a\rangle=\langle\kappa_a m_a\,|\,\boldsymbol{\sigma}\cdot\mathbf{Y}_{JLM}\,|\,\kappa_b m_b\rangle\ , \tag{A12}$$

where the second line follows because C_{JLM} is real. Now, it follows from Eqs. (A4a)–(A4c) that

$$\langle\kappa_a m_a\,|\,\boldsymbol{\sigma}\cdot\hat{\mathbf{r}}Y_{JM}\,|\,\kappa_b m_b\rangle=-I_{JM}(-\kappa_a m_a,\kappa_b m_b)\ , \tag{A13}$$

$$\langle\kappa_a m_a\,|\,\boldsymbol{\sigma}\cdot\mathbf{L}Y_{JM}\,|\,\kappa_b m_b\rangle=(\kappa_b-\kappa_a)I_{JM}(\kappa_a m_a,\kappa_b m_b)\ , \tag{A14}$$

$$\langle\kappa_a m_a\,|\,r\boldsymbol{\sigma}\cdot\boldsymbol{\nabla}Y_{JM}\,|\,\kappa_b m_b\rangle=(\kappa_b+\kappa_a)I_{JM}(-\kappa_a m_a,\kappa_b m_b)\ . \tag{A15}$$

It is now easy to solve, using Eqs. (A9) and (A12), for the basic coefficients C_{JLM},

$$C_{JJ+1M}=\left[\frac{J+1}{2J+1}\right]^{1/2}\left[1+\frac{\kappa_a+\kappa_b}{J+1}\right]\times I_{JM}(-\kappa_a m_a,\kappa_b m_b)\ ,$$

$$C_{JJM}=\frac{\kappa_b-\kappa_a}{\sqrt{J(J+1)}}I_{JM}(\kappa_a m_a,\kappa_b m_b)\ , \tag{A16b}$$

$$C_{JJ-1M}=\left[\frac{J}{2J+1}\right]^{1/2}\left[-1+\frac{\kappa_a+\kappa_b}{J}\right]\times I_{JM}(-\kappa_a m_a,\kappa_b m_b)\ . \tag{A16c}$$

APPENDIX B: APPLICATIONS TO THE BREIT INTERACTION

For small values of Z, the transverse interaction given in Eq. (1) can be expressed as a two-particle matrix element of the Breit interaction,[8]

$$B=-\frac{\alpha}{r_{12}}[\boldsymbol{\alpha}_1\cdot\boldsymbol{\alpha}_2-\tfrac{1}{2}(\boldsymbol{\alpha}_1\cdot\boldsymbol{\alpha}_2-\boldsymbol{\alpha}_1\cdot\hat{\mathbf{r}}_{12}\boldsymbol{\alpha}_2\cdot\hat{\mathbf{r}}_{12})]\ . \tag{B1}$$

This expression arises when the phase factor k_0 is omitted in Eq. (1) and is valid when (k_0r_{12}) is small compared to 1, as it is for low-Z atoms.

As an illustration of the utility of the developments in Appendix A, consider the evaluation of the integral

$$m_{abcd}\equiv-\int\frac{d^3r\,d^3r'}{|\mathbf{r}-\mathbf{r}'|}\psi^\dagger_{\kappa_a m_a}(\mathbf{r})\boldsymbol{\alpha}\psi_{\kappa_c m_c}(\mathbf{r})\cdot\psi^\dagger_{\kappa_b m_b}(\mathbf{r}')\times\boldsymbol{\alpha}\psi_{\kappa_d m_d}(\mathbf{r}')\ , \tag{B2}$$

which is an off-diagonal matrix element of the first term in the Breit interaction. First we notice that

$$\psi^{\dagger}_{\kappa_a m_a}(\mathbf{r})\alpha\psi_{\kappa_c m_c}(\mathbf{r}) = -\frac{i}{r^2}[g_a(r)f_c(r)\chi^{\dagger}_{\kappa_a m_a}(\Omega)\sigma\chi_{-\kappa_c m_c}(\Omega) - f_a(r)g_c(r)\chi^{\dagger}_{-\kappa_a m_a}(\Omega)\sigma\chi_{\kappa_c m_c}(\Omega)] . \quad \text{(B3)}$$

Using Eqs. (A16a)–(A16c) we introduce the following decomposition for Eq. (B3):

$$\psi^{\dagger}_{\kappa_a m_a}(\mathbf{r})\alpha\psi_{\kappa_c m_c}(\mathbf{r}) = -\frac{i}{r^2}\sum_{J,L,M}\mathbf{Y}_{JLM}(\Omega)C^{ac}_{JLM}(r) , \quad \text{(B4)}$$

with

$$C^{ac}_{JJ+1M} = \left[\frac{J+1}{2J+1}\right]^{1/2} I_{JM}(\kappa_c m_c,\kappa_a m_a)Q_{ca}(r) , \quad \text{(B5a)}$$

$$C^{ac}_{JJM} = \frac{\kappa_c+\kappa_a}{[J(J+1)]^{1/2}} I_{JM}(-\kappa_c m_c,\kappa_a m_a)V_{ca}(r) , \quad \text{(B5b)}$$

$$C^{ac}_{JJ-1M} = \left[\frac{J}{2J+1}\right]^{1/2} I_{JM}(\kappa_c m_c,\kappa_a m_a)P_{ca}(r) , \quad \text{(B5c)}$$

where we have defined

$$P_{ca}(r) = U_{ca} + \frac{\kappa_a-\kappa_c}{J}V_{ca} , \quad \text{(B6a)}$$

$$Q_{ca}(r) = -U_{ca} + \frac{\kappa_a-\kappa_c}{J+1}V_{ca} , \quad \text{(B6b)}$$

$$U_{ca} = g_c(r)f_a(r) - f_c(r)g_a(r) , \quad \text{(B6c)}$$

$$V_{ca} = g_c(r)f_a(r) + f_c(r)g_a(r) . \quad \text{(B6d)}$$

Inserting this expansion into Eq. (B2) and carrying out the partial-wave decomposition of $1/|\mathbf{r}-\mathbf{r}'|$ then leads to

$$m_{abcd} = -\sum_{l,m}\frac{4\pi}{2l+1}\sum_{J_1,L_1,M_1}\sum_{J_2,L_2,M_2}\int dr\,dr'\frac{r^l_<}{r^{l+1}_>}C^{ac}_{J_1L_1M_1}(r)C^{db}_{J_2L_2M_2}(r') \times \int d\Omega\mathbf{Y}^{\dagger}_{J_1L_1M_1}(\Omega)Y_{lm}(\Omega)\cdot\int d\Omega' Y^{*}_{lm}(\Omega')\mathbf{Y}_{J_2L_2M_2}(\Omega') . \quad \text{(B7)}$$

Carrying out the angular integration leads to the expression

$$m_{abcd} = -\sum_{J,L,M}\frac{4\pi}{2L+1}\int dr\,dr'\frac{r^L_<}{r^{L+1}_>}C^{ac}_{JLM}(r)C^{db}_{JLM}(r') . \quad \text{(B8)}$$

For each J there are contributions from three possible L values, each of which involves a radial integral and an angular factor that can be treated with the same techniques as those applied to the Coulomb interaction. One obtains

$$m_{abcd} = \sum_J J_J(abcd)[M_J(abcd)+N_J(abcd)] , \quad \text{(B9)}$$

$$J_J(abcd) = \sum_M(-1)^{j_a+j_b+J-m_a-m_b-M}\begin{pmatrix} j_a & J & j_c \\ -m_a & M & m_c\end{pmatrix}\begin{pmatrix} j_b & J & j_d \\ -m_b & -M & m_d\end{pmatrix} , \quad \text{(B10)}$$

$$M_J(abcd) = (-1)^J C_J(ac)C_J(bd)\left[\frac{J+1}{2J+3}\int_0^{\infty}dx\int_0^{\infty}dy\frac{x^{J+1}_<}{x^{J+2}_>}Q_{ac}(x)Q_{bd}(y) + \frac{J}{2J-1}\int_0^{\infty}dx\int_0^{\infty}dy\frac{x^{J-1}_<}{x^{J}_>}P_{ac}(x)P_{bd}(y)\right] , \quad \text{(B11)}$$

$$N_J(abcd) = (-1)^{J+1}C_J(-ac)C_J(-bd)\frac{(\kappa_a+\kappa_c)(\kappa_b+\kappa_d)}{J(J+1)}\int_0^{\infty}dx\int_0^{\infty}dy\frac{x^J_<}{x^{J+1}_>}V_{ac}(x)V_{bd}(y) . \quad \text{(B12)}$$

In Eq. (B11) the quantities $C_J(ab)$ are the reduced matrix elements defined in Eq. (A6), while the quantity $C_J(-ab)$ in Eq. (B12) is just $C_J(ab)$ with κ_a replaced by $-\kappa_a$, a change that modifies the parity selection rule only.

The extension of the above treatment to include the second term in the Breit interaction, Eq. (B1), is straightforward but lengthy; details can be found in Ref. 8. The result for second term in the Breit interaction matrix element is

$$r_{abcd} = \sum_J J_J(abcd)O_J(abcd) , \quad \text{(B13)}$$

$$O_J(abcd)=(-1)^{J+1}C_J(ac)C_J(bd)\left[\frac{(J+1)^2}{(2J+3)(2J+1)}\int_0^\infty dx\int_0^\infty dy\frac{x_<^{J+1}}{x_>^{J+2}}Q_{ac}(x)Q_{bd}(y)\right.$$
$$+\frac{J^2}{(2J-1)(2J+1)}\int_0^\infty dx\int_0^\infty dy\frac{x_<^{J-1}}{x_>^{J}}P_{ac}(x)P_{bd}(y)$$
$$+\frac{J(J+1)}{2(2J+1)}\int_0^\infty dx\int_0^x dy\left[\frac{x_<^{J-1}}{x_>^{J}}-\frac{x_<^{J+1}}{x_>^{J+2}}\right]Q_{ac}(x)P_{bd}(y)$$
$$\left.+\frac{J(J+1)}{2(2J+1)}\int_0^\infty dx\int_0^x dy\left[\frac{x_<^{J-1}}{x_>^{J}}-\frac{x_<^{J+1}}{x_>^{J+2}}\right]Q_{bd}(x)P_{ac}(y)\right]. \tag{B14}$$

The entire Breit interaction is given by the sum of these two parts

$$b_{abcd}=m_{abcd}+r_{abcd}\ . \tag{B15}$$

APPENDIX C: ANGULAR REDUCTION OF $E^{(3)}$

To facilitate the angular reduction of $E^{(3)}$, we introduce antisymmetrized Coulomb matrix elements $\tilde{g}_{abcd}$ defined by

$$\tilde{g}_{abcd}=g_{abcd}-g_{bacd}\ . \tag{C1}$$

Then in analogy to the standard radial reduction for g_{abcd},

$$\begin{aligned}
&g_{abcd}=\sum_L X_L(abcd)J_L(abcd)\ ,\\
&J_L(abcd)=\sum_M(-1)^{j_a+j_b+L-m_a-m_b-M}\begin{pmatrix}j_a & L & j_c\\ -m_a & M & m_c\end{pmatrix}\begin{pmatrix}j_b & L & j_d\\ -m_b & -M & m_d\end{pmatrix},\\
&X_L(abcd)=(-1)^L C_L(ac)C_L(bd)R_L(abcd)\ ,\\
&R_L(abcd)=\int dr_1dr_2\frac{r_<^L}{r_>^{L+1}}[g_a(r_1)g_c(r_1)+f_a(r_1)f_c(r_1)][g_b(r_2)g_d(r_2)+f_b(r_2)f_d(r_2)]\ ,
\end{aligned} \tag{C2}$$

where $C_L(ab)$ is defined in Appendix A, we find a corresponding reduction for $\tilde{g}_{abcd}$,

$$\begin{aligned}
&\tilde{g}_{abcd}=\sum_L Z_L(abcd)J_L(abcd)\ ,\\
&Z_L(abcd)=X_L(abcd)+[L]\sum_{L'}\begin{Bmatrix}j_b & j_d & L\\ j_a & j_c & L'\end{Bmatrix}X_{L'}(bacd)\ ,
\end{aligned} \tag{C3}$$

where $[L]=2L+1$. In deriving (C3) we have made use of the identity

$$J_L(bacd)=-\sum_{L'}[L']\begin{Bmatrix}j_b & j_d & L'\\ j_a & j_c & L\end{Bmatrix}J_{L'}(abcd)\ , \tag{C4}$$

which follows from an application of a theorem due to Jucys, Levinson, and Vanagas.[22]

The sums over magnetic quantum numbers in $E^{(3)}$ can now be performed using standard techniques. We find

$$E^{(3)}=\sum_{m,r,a,b,c}\sum_L(-1)^{j_a+j_b+j_c+j_m+j_r+j_v+L}\frac{1}{[j_v][L]^2}\frac{Z_L(carv)Z_L(mvba)Z_L(rbcm)}{(\varepsilon_v+\varepsilon_m-\varepsilon_a-\varepsilon_b)(\varepsilon_r+\varepsilon_v-\varepsilon_a-\varepsilon_c)}$$
$$-\sum_{a,c,n,m,r}\sum_L(-1)^{j_a+j_c+j_m+j_n+j_r+j_v+L}\frac{1}{[j_v][L]^2}\frac{Z_L(arnc)Z_L(cvrm)Z_L(mnva)}{(\varepsilon_m+\varepsilon_n-\varepsilon_a-\varepsilon_v)(\varepsilon_r+\varepsilon_m-\varepsilon_c-\varepsilon_v)}$$
$$+\sum_{n,m,a,b,c}\sum_{L_1,L_2}(-1)^{j_a+j_m+j_n+j_v+L_2}\frac{1}{[j_b][j_v][L_1]}\delta(j_b,j_c)\frac{Z_{L_1}(acmn)X_{L_1}(nmba)Z_{L_2}(vbcv)}{(\varepsilon_n+\varepsilon_m-\varepsilon_a-\varepsilon_b)(\varepsilon_n+\varepsilon_m-\varepsilon_a-\varepsilon_c)}$$
$$-\sum_{a,b,m,n,r}\sum_{L_1,L_2}(-1)^{j_a+j_b+j_n+j_v+L_2}\frac{1}{[j_r][j_v][L_1]}\delta(j_m,j_r)\frac{Z_{L_1}(abrn)X_{L_1}(nmba)Z_{L_2}(vrmv)}{(\varepsilon_n+\varepsilon_m-\varepsilon_a-\varepsilon_b)(\varepsilon_r+\varepsilon_n-\varepsilon_a-\varepsilon_b)}$$

$$
\begin{aligned}
&-\sum_{n,a,b,c,d}\sum_{L_1,L_2,L_3}\frac{1}{[j_v]}\begin{Bmatrix}L_2 & L_3 & L_1\\ j_a & j_c & j_n\end{Bmatrix}\begin{Bmatrix}L_2 & L_3 & L_1\\ j_b & j_d & j_v\end{Bmatrix}\frac{X_{L_1}(badc)Z_{L_2}(dcvn)X_{L_3}(vnba)}{(\varepsilon_v+\varepsilon_n-\varepsilon_a-\varepsilon_b)(\varepsilon_v+\varepsilon_n-\varepsilon_c-\varepsilon_d)}\\
&+\sum_{a,n,m,r,s}\sum_{L_1,L_2,L_3}\frac{1}{[j_v]}\begin{Bmatrix}L_2 & L_3 & L_1\\ j_s & j_a & j_m\end{Bmatrix}\begin{Bmatrix}L_3 & L_1 & L_2\\ j_v & j_n & j_r\end{Bmatrix}\frac{Z_{L_1}(avsr)X_{L_2}(nmva)X_{L_3}(rsnm)}{(\varepsilon_n+\varepsilon_m-\varepsilon_a-\varepsilon_v)(\varepsilon_r+\varepsilon_s-\varepsilon_a-\varepsilon_v)}\\
&+2\sum_{n,r,a,b,c}\sum_{L}(-1)^{j_a+j_b+j_c+j_n+j_r+j_v+L}\frac{1}{[j_v][L]^2}\frac{Z_L(acnr)Z_L(nvab)Z_L(rbcv)}{(\varepsilon_n+\varepsilon_v-\varepsilon_a-\varepsilon_b)(\varepsilon_r+\varepsilon_n-\varepsilon_a-\varepsilon_c)}\\
&-2\sum_{a,c,n,m,r}\sum_{L}(-1)^{j_a+j_c+j_m+j_n+j_r+j_v+L}\frac{1}{[j_v][L]^2}\frac{Z_L(carm)Z_L(nmva)Z_L(vrnc)}{(\varepsilon_m+\varepsilon_n-\varepsilon_a-\varepsilon_v)(\varepsilon_r+\varepsilon_m-\varepsilon_c-\varepsilon_a)}\\
&+2\sum_{r,m,a,c,d}\sum_{L_1,L_2}(-1)^{j_c+j_d+j_r+j_v+L_2}\frac{1}{[j_a][j_v][L_1]}\delta(j_a,j_m)\frac{Z_{L_1}(dcrm)Z_{L_2}(mvva)X_{L_1}(radc)}{(\varepsilon_m-\varepsilon_a)(\varepsilon_r+\varepsilon_m-\varepsilon_c-\varepsilon_d)}\\
&-2\sum_{m,r,s,a,c}\sum_{L_1,L_2}(-1)^{j_c+j_r+j_s+j_v+L_2}\frac{1}{[j_a][j_v][L_1]}\delta(j_a,j_m)\frac{Z_{L_1}(casr)Z_{L_2}(mvva)X_{L_1}(rsmc)}{(\varepsilon_m-\varepsilon_a)(\varepsilon_r+\varepsilon_s-\varepsilon_c-\varepsilon_a)}\\
&-2\sum_{a,b,s,m,r}\sum_{L_1,L_2,L_3}\frac{1}{[j_v]}\begin{Bmatrix}L_2 & L_3 & L_1\\ j_b & j_s & j_v\end{Bmatrix}\begin{Bmatrix}L_3 & L_2 & L_1\\ j_r & j_a & j_m\end{Bmatrix}\frac{Z_{L_1}(basr)X_{L_2}(rsmv)X_{L_3}(vmba)}{(\varepsilon_v+\varepsilon_m-\varepsilon_a-\varepsilon_b)(\varepsilon_r+\varepsilon_s-\varepsilon_a-\varepsilon_b)}\\
&+2\sum_{n,m,a,c,d}\sum_{L_1,L_2,L_3}\frac{1}{[j_v]}\begin{Bmatrix}L_1 & L_2 & L_3\\ j_a & j_c & j_m\end{Bmatrix}\begin{Bmatrix}L_2 & L_3 & L_1\\ j_d & j_n & j_v\end{Bmatrix}\frac{Z_{L_1}(cdmn)X_{L_2}(nmva)X_{L_3}(vadc)}{(\varepsilon_n+\varepsilon_m-\varepsilon_a-\varepsilon_v)(\varepsilon_n+\varepsilon_m-\varepsilon_c-\varepsilon_d)}\,.
\end{aligned}
\tag{C5}
$$

An alternative approach is to multiply out the parentheses in Eq. (6), giving 56 distinct terms, and to perform an angular separation for each term separately. As a cross check, we have also developed codes based on this approach, and obtain precise agreement with codes based on Eq. (C5). The angular factors in Eq. (C5) were determined with the aid of a program written in the symbolic language REDUCE.[23]

[1]P. G. H. Sandars, Phys. Scr. **36**, 904 (1987).

[2]S. P. Goldman and G. W. F. Drake, J. Phys. B **17**, L197 (1984).

[3]J. Hata and I. P. Grant, J. Phys. B **17**, 931 (1984).

[4]P. J. Mohr, Phys. Rev. A **32**, 1949 (1985).

[5]I. Lindgren, Phys. Rev. A **31**, 1273 (1985). Calculations of the lithium isoelectronic sequence have been given by K. T. Cheng, Y.-K. Kim, and J. P. Desclaux, At. Data Nucl. Data Tables **24**, 111 (1979) and by U. I. Safronova, J. Quant. Spec. and Rad. Transfer **15**, 231 (1975).

[6]J. Sapirstein, Phys. Scr. **36**, 801 (1987); see also I. P. Grant and H. M. Quiney, Adv. Atom. Mol. Phys. (to be published).

[7]J. B. Mann and W. R. Johnson, Phys. Rev. A **4**, 41 (1971).

[8]In the present paper we use the values of this function given in Table II in W. R. Johnson and Gerhard Soff, At. Data Nucl. Data Tables **33**, 405 (1985); see also P. J. Mohr, *ibid.* **29**, 453 (1983).

[9]W. R. Johnson, M. Idrees, and J. Sapirstein, Phys. Rev. A **35**, 3218 (1987).

[10]J. Sucher, Int. J. Quantum Chem. **25**, 3 (1984).

[11]G. E. Brown and D. E. Ravenhall, Proc. R. Soc. London, Ser. A **208**, 552 (1951).

[12]P. K. Kabir and E. E. Salpeter, Phys. Rev. **108**, 1256 (1957).

[13]S. A. Blundell, D. S. Guo, W. R. Johnson, and J. Sapirstein, At. Data Nucl. Data Tables **37**, 103 (1987).

[14]D. S. Hughes and Carl Eckart, Phys. Rev. **36**, 694 (1930).

[15]B. Edlén, Phys. Scr. **28**, 51 (1983); B. Denne and E. Hinnov, *ibid.* **35**, 811 (1987).

[16]J. P. Desclaux, Comput. Phys. Commun. **9**, 31 (1975).

[17]I. P. Grant, B. J. McKenzie, P. H. Norrington, D. F. Mayers, and N. C. Pyper, Comput. Phys. Commun. **21**, 207 (1980).

[18]A. M. Desiderio and W. R. Johnson, Phys. Rev. A **3**, 1267 (1971).

[19]S. D. Lakdawala and P. J. Mohr, Phys. Rev. A **29**, 1047 (1984).

[20]P. J. Mohr (private communication).

[21]G. Adkins, Phys. Rev. D **34**, 2489 (1986).

[22]I. Lindgren and J. Morrison, *Atomic Many-Body Theory,* 2nd Ed. (Springer, Berlin, 1986), p. 85.

[23]REDUCE is described by A. C. Hearn (unpublished).